ACADEMIC PRESS

Available online at www.sciencedirect.com

SCIENCE DIRECT®

DEVELOPMENTAL BIOLOGY

Developmental Biology 258 (2003) 334–348

www.elsevier.com/locate/ydbio

Continuous loss of oocytes throughout meiotic prophase in the normal mouse ovary

Kelly A. McClellan,[a] Roger Gosden,[b] and Teruko Taketo[a,c,*]

[a] *Department of Biology, McGill University, Montreal, Quebec H3A 1B1, Canada*
[b] *Department of Obs/Gyn, McGill University, Montreal, Quebec H3A 1A1, Canada*
[c] *Urology Research Laboratory, Department of Surgery, McGill University, Montreal, Quebec H3A 1A1, Canada*

Received for publication 13 November 2002, revised 21 February 2003, accepted 27 February 2003

Abstract

The number of germ cells reaches the maximum just prior to entry into meiosis, yet decreases dramatically by a few days after birth in the female mouse, rat, and human. Previous studies have reported a major loss at the pachytene stage of meiotic prophase during fetal development, leading to the hypothesis that chromosomal pairing abnormalities may be a signal for oocyte death. However, the identification as well as the quantification of germ cells in these studies have been questioned. A recent study using Mouse Vasa Homologue (MVH) as a germ cell marker reached a contradictory conclusion claiming that oocyte loss occurs in the mouse only after birth. In the present study, we established a new method to quantify murine germ cells by using Germ Cell Nuclear Antigen-1 (GCNA-1) as a germ cell marker. Comparison of GCNA-1 and MVH immunolabeling revealed that the two markers identify the same population of germ cells. However, nuclear labeling of GCNA-1 was better suited for counting germ cells in histological sections as well as for double labeling with the antibody against synaptonemal complex (SC) proteins in chromosome spreading preparations. The latter experiment demonstrated that the majority of GCNA-1-labeled cells entered and progressed through meiotic prophase during fetal development. The number of GCNA-1-positive cells in the ovary was estimated by counting the labeled cells retained in chromosome spreading preparations and also in histological sections by using the ratio estimation method. Both methods demonstrated a continuous decline in the number of GCNA-1-labeled cells during fetal development when the oocytes progress through meiotic prophase. These observations suggest that multiple causes are responsible for oocyte elimination.

Keywords: Mouse fetal ovary; Germ cell; Oocyte; GCNA-1; MVH; Meiotic prophase

Introduction

Since female germ cells only enter meiosis during fetal life, the initial endowment of oocytes is a limiting factor of the reproductive life span. Moreover, the oocyte population is continuously reduced throughout reproductive life, leaving only a small percentage of the initial oocyte endowment available for ovulation and fertilization. The cause as well as the biological significance of oocyte elimination remains largely unknown (reviewed by Tilly, 2001).

Classical studies have shown a major loss of mammalian oocytes occuring before birth (Beaumont and Mandl, 1962; Baker, 1963; Burgoyne and Baker, 1985). The number of rat oocytes, identified by morphological criteria, was shown to decrease by two-thirds from the onset of meiosis to 2 days after birth, when the majority of oocytes become arrested at the end of meiotic prophase (Beaumont and Mandl, 1962). Light and electron microscope studies revealed three distinct morphological features of degenerating germ cells in the ovary (Beaumont and Mandl, 1962; Franchi and Mandl, 1962). The first, termed “atretic divisions,” denotes the oogonia that appear to be in mitotic metaphase while lacking visible spindles. The second, termed “Z cells,” are the oocytes that appear to be in meiotic prophase with abnormal chromosome condensation and eosinophilic cytoplasm. The third denotes the oocytes that have the nuclear configuration of diplotene stage but with somewhat abnormal chromo-

* Corresponding author. Fax: +514-843-1457.
E-mail address: teruko.taketo@muhc.mcgill.ca (T. Taketo).

0012-1606/03/$ – see front matter © 2003 Elsevier Science (USA). All rights reserved.
doi:10.1016/S0012-1606(03)00132-5

some condensation and crinkling of the nuclear membrane. Analogous studies in human ovaries have demonstrated similar morphological features of degenerating oogonia and oocytes and a reduction in the oocyte population in fetal life was estimated to be more than 70% (Baker, 1963; Baker and Franchi, 1967).

In the mouse ovary, several authors have noted degenerating oogonia, a significant number of degenerating pachytene oocytes, and degenerating diplotene oocytes (Borum, 1961; Bakken and McClanahan, 1978). More recent studies with the electron microscope have demonstrated the oogonia arrested in mitotic metaphase but lacking spindles (Wartenberg et al., 2001). Silver staining of air-dried oocytes has demonstrated that 25% of pachytene oocytes have gaps in synaptonemal complex (SC) regions, interpreted as a sign of degeneration (Speed, 1982). The change in the total oocyte population throughout ovarian development was not examined in these studies. Burgoyne and Baker (1985) have shown a sharp decline in the germ cell population in prenatal, as well as neonatal, mouse ovaries. However, their morphological criteria for defining germ cells are unclear. Pepling and Spradling (2001) have recently used an antibody against Mouse Vasa Homologue (MVH) to identify the oocyte and reported that the decrease in the oocyte population is limited to the neonatal period, between 1 and 2 days after birth. This finding contradicts the previous studies, as well as the morphological observations of degenerating oocytes in the fetal mouse ovary. Three explanations are conceivable. First, the fate of oocytes may be different between the mouse and other mammalian species. Second, the anti-MVH antibody may recognize a population of cells that differ from the "oocytes" defined in the earlier morphological studies. Since the morphological criteria for identifying an oocyte under the light microscope relies on nuclear condensation, it is possible that errors could have been made in defining oocytes. For example, germ cells not in meiosis may be excluded, whereas somatic cells in mitotic metaphase may be included as oocytes. As well, degenerating cells may have been counted as oocytes. Third, the estimation method used by Pepling and Spradling may not have fully represented the total population of MVH labeled cells. As a single "representative" section was counted in each ovary, bias may have been imposed in choosing the section, or counting one section may not represent the entire ovary.

The timing of major germ cell loss during ovarian development is critical for judging the causes of germ cell elimination. Indeed, the hypotheses that have been proposed to explain germ cell elimination point toward its occurrence during discrete developmental periods. First, limited amounts of trophic factors may permit the survival of only a fraction of germ cells. Cytokines and growth factors, such as leukemia inhibitory factor (LIF), retinoic acid (RA), and stem cell factor (SCF), have been shown to prevent loss of germ cells in culture (Godin et al., 1991; Matsui et al., 1991; Resnick et al., 1992; Dolci et al., 1993; Pesce et al., 1993; Koshimizu et al., 1995; Morita and Tilly, 1999). Furthermore, in vivo roles for mast cell growth factor (MGF = SCF) and its receptors have been confirmed by germ cell deficiency in their respective mutant mice (Mintz and Russell, 1957; Chabot et al., 1988; Huang et al., 1990; Zsebo et al., 1990; Brannan et al., 1991). These trophic factors likely influence the oocyte populations equally at various stages of meiotic prophase. Second, germ cells with telomere dysfunction may be recognized at the onset of meiosis and thereby eliminated. It has recently been found that, in late generations of telomerase-deficient mice, the proportion of germ cells with dysfunctional telomeres, relative to that of somatic cells, drops after the onset of meiosis (Hemann et al., 2001). Third, errors in chromosome pairing during meiotic prophase may trigger oocyte elimination. This hypothesis has been proposed because morphological features of degenerating oocytes have often been seen when the majority of oocytes reach the pachytene stage of meiotic prophase (Speed, 1982, 1988; Dietrich and Mulder, 1983; Mittwoch and Mahadevaiah, 1992). Furthermore, various mutations of genes involved in homologous pairing and DNA repair block the progress of meiotic prophase (Baker et al., 1996; Edelmann et al., 1996; 1999; Pittman et al., 1998; Kneitz et al., 2000). In these cases, a major oocyte loss must follow the peak of pachytene stage (Burgoyne and Baker, 1985; Burgoyne et al., 1985). Finally, the massive reduction in oocytes may serve a more altruistic purpose. It has been proposed that the dying oocytes may play an important role by donating their cytoplasmic components, such as mitochondria, to the surviving oocytes within a cyst (Pepling and

Fig. 1. Comparison of GCNA-1 and MVH immunolabeling in histological sections (A–F) and dissociated cells (G–L) from ovaries at DOB. (A) An ovarian section labeled with the anti-GCNA-1 antibody. The labeled cells are concentrated at the periphery and scarce in the central region. Scale bar, 100 μm. (B, C) High magnification of the section shown in (A), dually stained with DAPI (B) and with the anti-GCNA-1 antibody (C). The cells showing morphological characteristics of oocytes with DAPI staining (arrowheads in B) are labeled for GCNA-1 in the nucleus (arrowheads in C). (D) The adjacent section of that shown in (A), labeled with the anti-MVH antibody. Distribution of the MVH labeled cells is similar to that of the GCNA-1-labeled cells. Scale bar, 100 μm. (E, F) High magnification of the section shown in (D), dually stained with DAPI (E) and with the anti-MVH antibody (F). The cells showing morphological characteristics of oocytes with DAPI staining (arrowheads in E) are labeled for MVH in the cytoplasm (arrowheads in F). Scale bar, 25 μm (also for B, C, and E). (G) Dissociated ovarian cells labeled with the anti-GCNA-1 antibody. The labeling is localized in the nucleus. (H) The ovarian cells shown in (G), labeled with the anti-MVH antibody. Note two populations of MVH-labeled cells. Those labeled exclusively in the cytoplasm are also labeled for GCNA-1 (G), whereas those labeled in the nucleus (arrowhead), as identified by DAPI staining (data not shown), are negative for GCNA-1. (I) Overlay of (G) and (H). GCNA-1-labeled cells in (G) overlap only with the MVH-labeled cells in the cytoplasm in (H). Scale bar, 50 μm (also for G and H). (J) An ovarian cell labeled with the anti-GCNA-1 antibody in the nucleus shown at a high magnification. (K) The same cell shown in (J) labeled with the anti-MVH antibody. The cytoplasm is evenly labeled. (L) Overlay of (J) and (K). Scale bar, 10 μm (also for J and K).

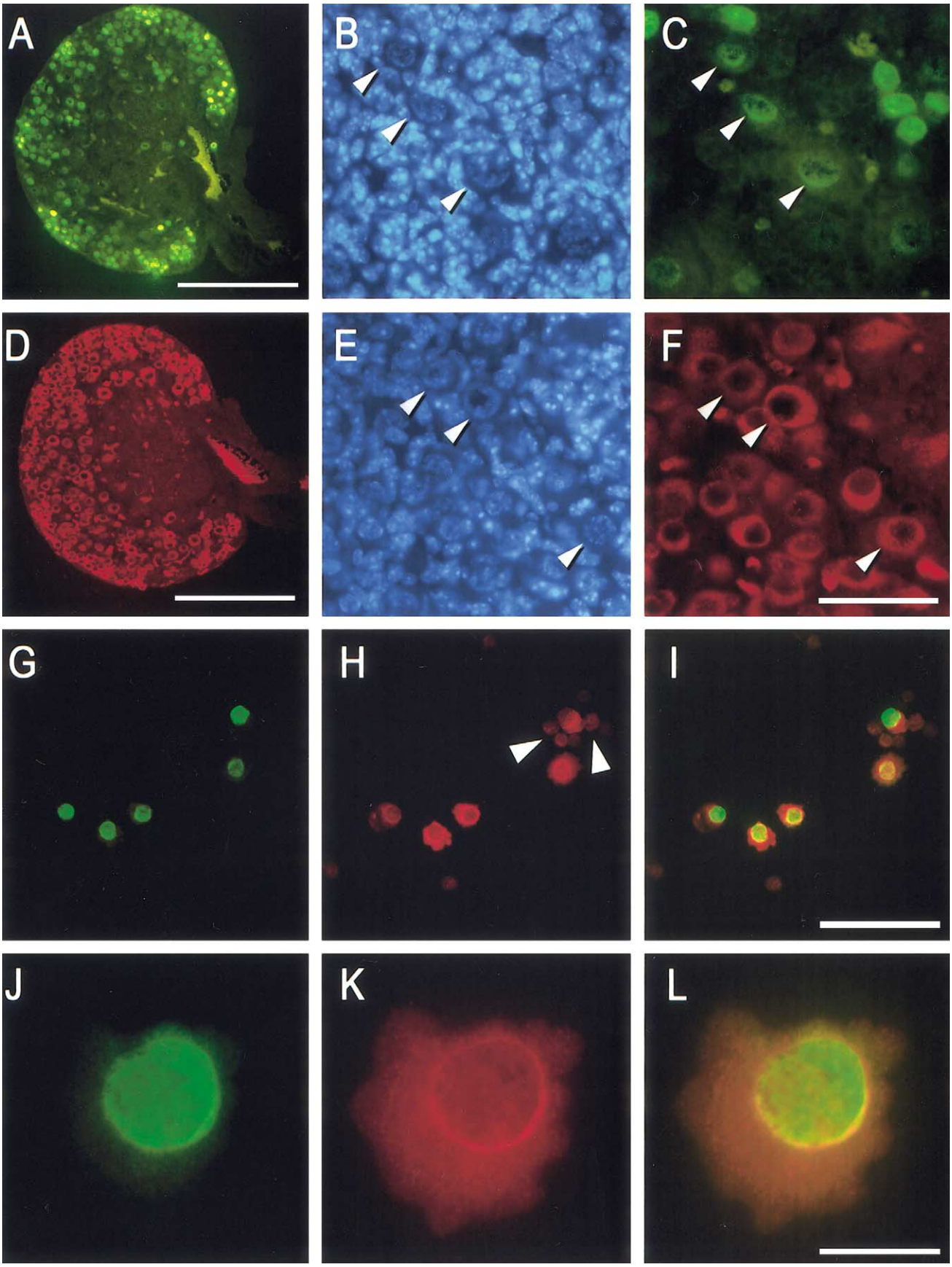
A
B
C
D
E
F
G
H
I
J
K
L

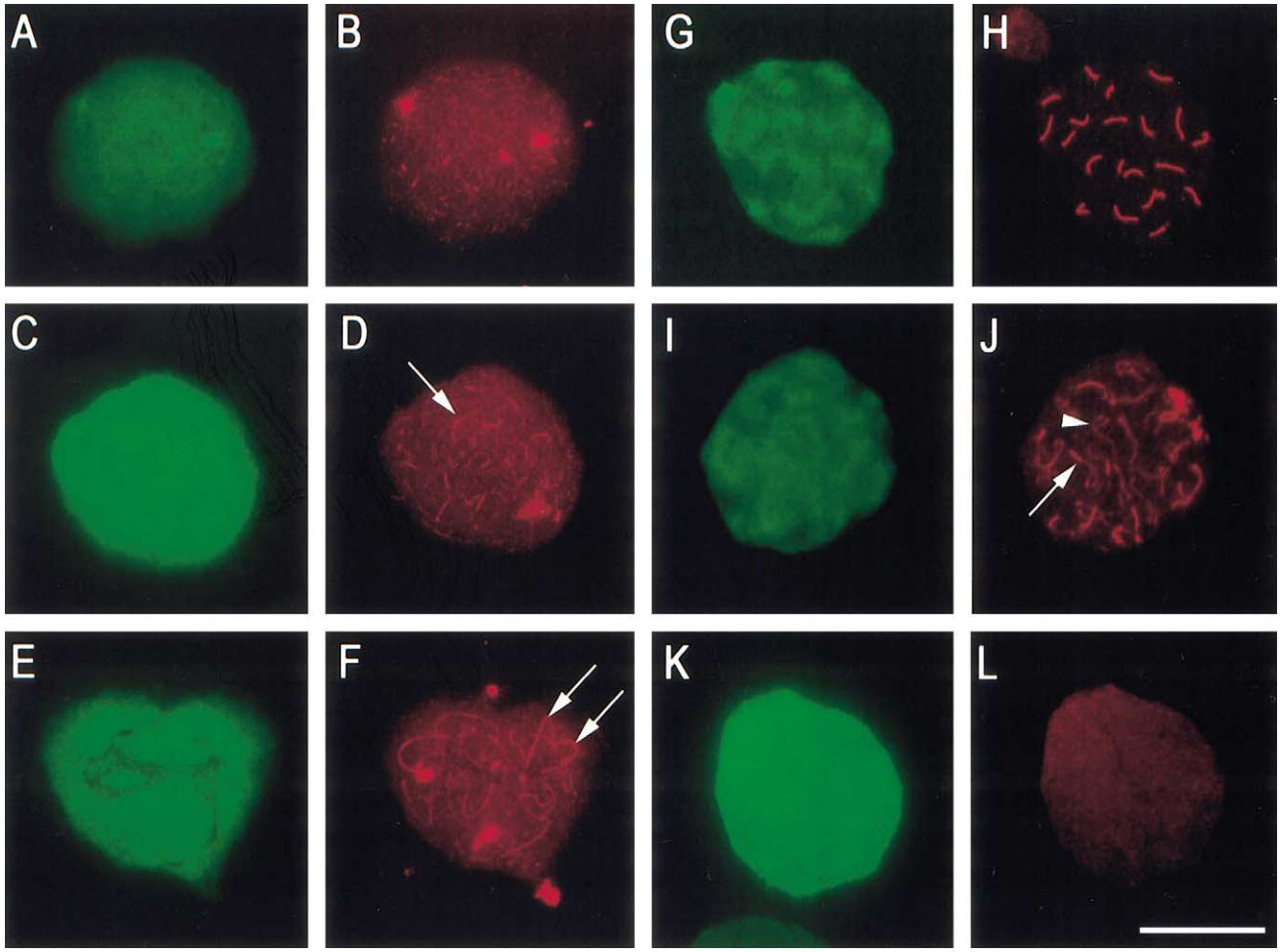

Fig. 2. Stages of meiotic prophase as identified by SC labeling patterns (B, D, F, H, J, and L) in GCNA-1-labeled cells (A, C, E, G, I, and K) in chromosome spreading preparations. Scale bar, 10 μm. (A, B) Leptotene oocyte at 14.5 dpc is characterized by diffuse fine threadlike SC immunolabeling over the nucleus. (C, D) Early zygotene oocyte at 15.5 dpc is characterized by apparent thickening of SC labeling at discrete loci (arrow), representing the beginning of homologous pairing. (E, F) Mid zygotene oocyte at 15.5 dpc is characterized by elongation of the thick SC labeling at the homologous pairing cores (arrows). (G, H) Mid pachytene oocyte at 18.5 dpc is characterized by the presence of 20 discrete SC labeled threads, representing the homologous pairing along the entire length. (I, J) Early diplotene oocyte at DOB is characterized by the appearance of "Y"-shaped structures with SC labeling (arrowhead) stretching from the thick thread (arrow). This feature represents the beginning of dissociation between the homologous pairs. (K, L) GCNA-1-labeled cell at DOB with the background level of SC immunolabeling, named "complex negative."

Spradling, 2001). This hypothesis is based on the observation that a major loss of oocytes occurs after birth, when oocyte cysts break down into individual cells.

The present study aimed to establish a reliable new method to quantify murine oocytes and to determine the gestational age and meiotic prophase stage at which major oocyte loss occurs. First, we compared two markers for germ cells to identify oocytes. Although several germ cell markers have been identified, only two, Germ Cell Nuclear Antigen-1 (GCNA-1) and MVH, are expressed in oocytes through fetal to early postnatal life (Enders and May, 1994; Fujiwara et al., 1994; Pesce et al., 1998; Toyooka et al., 2000). A rat monoclonal anti-GCNA-1 antibody has been raised against enriched mouse pachytene spermatocytes (Enders and May, 1994). The antigen is expressed specifically in primordial germ cells upon entry into fetal gonads, and the expression continues in the developing gonads of both sexes until late diplotene stage of meiotic prophase (Wang et al., 1997). The antibody recognizes a heterogeneous population of proteins between 80 and 110 kDa in spermatogenic cells, but the gene encoding the antigen has yet to be identified. A rabbit polyclonal anti-MVH antibody has been raised against full-length murine MVH protein, a member of the DEAD box family of RNA helicases (Toyooka et al., 2000). The antibody recognizes a single 85-kDa band in adult testis, corresponding to the known molecular weight of MVH protein (Fujiwara et al., 1994). Immunohistochemical studies have shown that MVH is expressed in germ cells upon their interaction with the somatic cells of gonadal primordia (Toyooka et al., 2000). The expression in oocytes continues throughout fetal development, persisting until the development of primordial follicles (Toyooka et al., 2000; Pepling and Spradling, 2001). We chose GCNA-1 as an appropriate marker for the present

study after comparing the immunolabeling profiles of both markers in ovarian sections and in dispersed cell preparations. Next, we examined whether the GCNA-1-labeled cells represent oocytes in meiotic prophase by double labeling with anti-GCNA-1 and anti-SC antibodies in chromosome spreading preparations. The characteristic immunolabeling pattern with the anti-SC antibody offers a reliable method for determining the stages of meiotic prophase (Heyting et al., 1988; Dobson et al., 1994; Schalk et al., 1998; Amleh et al., 2000). Finally, we counted the numbers of GCNA-1-labeled cells retained in chromosome spreading preparations from each pair of ovaries, and estimated the total number of GCNA-1 labeled cells in each ovary using the ratio estimation method in histological sections throughout fetal and neonatal development. The results reveal a continuous decrease in the oocyte population throughout meiotic prophase.

Materials and methods

Isolation of ovaries

All animal procedures were performed in accordance with the Canadian Council on Animal Care and approved by the McGill University Animal Care Committee. Adult CD-1 males (Charles River Canada, St. Constant, Quebec) were caged with adult CD-1 females overnight, and the presence of vaginal plugs was examined the following mornings between 09:00 and 11:00 for up to 3 days. Females with vaginal plugs were removed and caged separately until use. Under the assumption that mating occurred between 00:00 and 02:00, the next midday was defined as 0.5 days postcoitum (dpc). Pregnant females were sacrificed by cervical dislocation between 13.5 and 18.5 dpc, and their fetuses were removed from the uterine horns. Ovaries were removed from the fetuses and freed from the surrounding tissue in Minimal Essential Medium containing Hank's salts and 25 mM Hepes buffer (MEM [H]) (Gibco Invitrogen Corporation, Burlington, ON) under a dissecting microscope (Wild, Heerburg, Switzerland). Neonatal ovaries were similarly obtained from the litters delivered by pregnant CD-1 females. As pups were born on 19.5 dpc, this day was defined as day of birth (DOB), and the following day was defined as 1 day postpartum (dpp). Neonatal ovaries were collected from DOB to 3 dpp. The isolated ovaries were either immediately fixed for paraffin embedding or processed for chromosome spreading and/or dispersed cell preparations.

Histological preparations

Ovaries were fixed in a 3:1 fresh mixture of absolute ethanol and acetic acid for 1 h at room temperature (RT), rinsed, and stored in 70% ethanol at 4°C until embedding. Tissues were dehydrated through gradient concentrations of ethanol and toluene at RT. Tissues were then infiltrated in a mixture of 1:1 toluene and melted paraffin (Paraplast Plus, Fisher Scientific Canada, Montreal, Quebec), followed by two changes in paraffin alone at 60°C. The tissues were finally embedded in melted paraffin, and the paraffine blocks were stored at 4°C. The entire ovary embedded in paraffin was sectioned at 5 μm thickness. For GCNA-1 labeling, 10 sequential sections were placed on each microscope slide (VWR Scientific, West Chester, PA). For GCNA-1 and MVH parallel labeling, sequential sections were alternated between two slides.

Preparation of dispersed cells and chromosome spreading

The conventional method to prepare chromosome spreading from fetal ovaries has been described previously (Amleh et al., 2000). A cytospin centrifugation step was introduced when the cell suspension was applied to histological slides and carried out according to the manufacturer's instruction (Thermo IEC, Needham Heights, MA). Briefly, the bottoms of cytospin chambers were coated with vacuum grease (Dow Corning, Midland, MI) and placed on positively charged histology slides (Fisher Scientific Canada). A total of 400 μl of 0.5% hypotonic NaCl solution (pH 8.2) was added to each chamber, and the cell suspension was dropped onto the top. The cells in chambers were allowed to settle for 5 min at RT, and then centrifuged for 5 min at 500*g* at RT. The supernatant was aspirated out of the chambers, and 200 μl of 2% paraformaldehyde (pH 8.2) was added to each chamber. The chambers were centrifuged for 30 s at 100*g* at RT. This process was repeated once more with fixative and three times for washing with 0.4% Photo-Flo (Kodak Canada, Toronto, ON) (pH 8.0). The slides were removed from the chambers, air-dried under vacuum for 10 min, and either processed immediately for immunocytochemistry, or stored in an airtight container with silica gel at −20°C for subsequent use.

As the hypotonic treatment and subsequent centrifugation usually disrupted the cell membrane, a modification was introduced to preserve the cytoplasmic structures for double labeling of MVH and GCNA-1. The method for preparing cell suspensions was identical to that described for the conventional method. After the final centrifugation, the cells were resuspended in 200 μl of 2% paraformaldehyde in PBS (pH 7.6). After 10 s of gentle pipetting, the cells were centrifuged for 3 min at 380*g* at RT. This fixation process was repeated once more. The cells were then resuspended in 16 μl of PBS, and added directly to histology slides under chambers and centrifuged, followed by three times washings as described above.

Fluorescent immunocytochemical labeling

Histological sections on slides were deparaffinized by toluene and rehydrated through decreasing concentrations of ethanol. The deparaffinized slides as well as the slides

with chromosome spreading were washed three times each for 10 min in the Antibody Dilution Buffer (ADB) containing PBS (pH 7.6), 1% normal goat serum (Gibco Invitrogen Corporation, Groningen, the Netherlands), 0.3% bovine serum albumin, and 0.005% Triton X-100 (both Sigma-Aldrich Canada, Oakville, ON). The slides were then incubated overnight in a humid chamber at RT with the rat IgM monoclonal anti-GCNA-1 antibody at a concentration of 1:50 and the rabbit anti-SC (or anti-MVH) antibody at a concentration of 1:1000, diluted in ADB. The next day, the slides were washed in ADB (3×10 min) and incubated for 45 min with the goat anti-rat IgM fluorescein isothiocyanate (FITC) conjugated (Pierce Endogen, Rockford, IL) and the goat anti-rabbit IgG biotin conjugated (Pierce Endogen), both diluted to 1:1000 in ADB. The slides were washed in ADB (3×10 min) and incubated for 30 min with the avidin -Cy3 conjugated (Pierce Endogen) at a final concentration of 1:1000 in ADB. The slides were washed in PBS (3×10 min), followed by double distilled water (2×2 min), and air-dried under vacuum for 10 min. The slides were mounted in the Prolong Antifade mounting medium prepared according to the manufacturer's instruction (Molecular Probes, Eugene, OR) and supplemented with 0.4 μg/mL 4′,6-diamidine-2′-phenylindole dihydrochloride (DAPI) (Boehringer Mannheim, Germany). All slides were examined under a fluorescence microscope (Zeiss Axiophot, Germany). Immunocytochemical controls were performed in parallel by processing slides as described above with the omission of primary antibodies. In addition, the absence of cross-reactivity of the secondary antibodies was verified by incubating the slides with the noncorresponding secondary antibodies. All images were captured with a digital camera (Retiga 1300, QImaging, Burnaby, BC) and processed with Northern Eclipse digital imaging software, version 6.0 (Empix Imaging, Mississauga, ON) on an IBM compatible computer. Acquired images were further processed with Adobe Photoshop version 6.0 (Adobe Systems Inc., San Jose, CA).

The rat monoclonal anti-GCNA-1 antibody was a gift from Dr. G. Enders, University of Kansas, Kansas City, KS (Enders and May, 1994). The rabbit polyclonal anti-MVH antibody was a gift from Dr. T. Noce, Mitsubishi-Kasei Institute of Life Sciences, Tokyo, Japan (Toyooka et al., 2000). The rabbit polyclonal anti-SC antibody was a gift from Dr. P. Moens, York University, Toronto, ON (Dobson et al., 1994).

Counting of GCNA-1-immunolabeled cells in chromosome spreading preparations

The total number of GCNA-1-labeled cells retained on a slide was counted under a microscope at a low magnification (200×). With the conventional method, two or three pairs of ovaries were examined from two litters at each gestation age. With the cytospin method, a total of six pairs of ovaries were examined from a minimum of two litters at each gestation age.

The proportions of GCNA-1-labeled cells in meiotic prophase stages were determined in representative fields of slides with chromosome spreading prepared by the cytospin method. The area containing cells on each slide was divided into 4 quadrants, in each of which the fields of view were arbitrarily chosen. All GCNA-1-labeled cells in a selected field were counted and assessed for their SC immunolabeling profiles at a higher magnification (400 and 1000×). The counting was continued until a minimum of 25 GCNA-1-labeled cells was scored in each quadrant, and thus over 100 cells per pair of ovaries. The meiotic prophase stages were determined by characteristic patterns of SC immunolabeling. The percentages of individual meiotic prophase stages were averaged among 6 pairs of ovaries at each gestation age.

Immunolabeling of GCNA-1 in histological sections

Slides were deparaffinized and incubated with the rat monoclonal anti-GCNA-1 antibody overnight, followed by the goat anti-rat IgM biotin conjugated, as described above. After washings, the slides were incubated for 30 min at RT with the avidin–biotin–horseradish–peroxidase complex according to the manufacturer's instruction (ABC Vectastain Kit, Vector Laboratories, Burlingame, CA). After washings in PBS (3×10 min), the slides were incubated for 6 min in a solution of 0.02% 3′3-diaminobenzidine (DAB) and 0.005% H_2O_2 in 0.05 M Tris buffer, pH 7.5 (Sigma-Aldrich Canada), and rinsed in PBS. The slides were then dehydrated through gradient concentrations of ethanol, cleared in toluene, and mounted in Permount mounting medium (Fisher Scientific Canada). Immunocytochemical controls were performed in parallel by processing slides as described above with omission of the anti-GCNA-1 antibody. The slides were observed under a light microscope (Zeiss Axiophot).

Estimation of the total number of GCNA-1-immunolabeled cells per ovary in histological sections

The ratio estimation method (Levy and Lemeshow, 1999) with modifications was used to obtain the total number of GCNA-1-labeled cells in the ovary. All labeled cells were counted in randomly selected sections representing approximately 10% (5–7 sections) of each ovary. Random numbers were generated with Microsoft Excel 97 (Microsoft Corporation, Seattle, WA). The picture of the entire ovary section at low magnification (200×) was captured with a digital camera (Retiga 1300, QImaging), and all GCNA-1-labeled cells in the section were counted with the manual count application on Northern Eclipse imaging software, version 6.0 (Empix). The area of the section was also measured from the digital image with the area measurement application in Northern Eclipse imaging software. From these values, the average number of GCNA-1-labeled cells

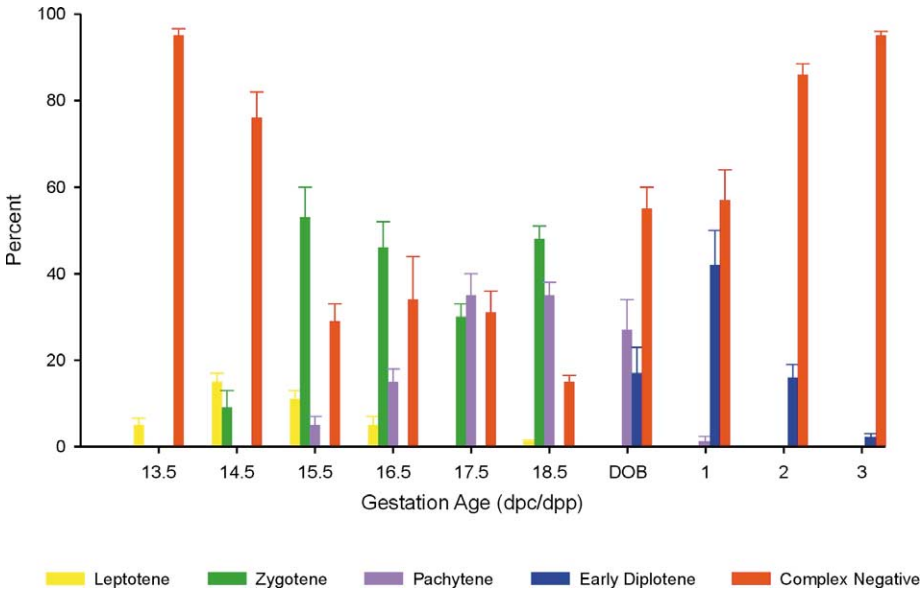

Fig. 3. Progress of meiotic prophase in GCNA-1-labeled cells. Each meiotic prophase stage represents the proportion of total cells (mean ± SEM) obtained from six pairs of ovaries from two litters at each gestation age.

to area ratio was calculated. This ratio was multiplied by a calculated estimate of the total ovary area. To estimate the total ovary area, the area of every fifth section was measured, the mean section area was calculated, and multiplied by the total number of sections cut from the ovary. The average number of GCNA-1-labeled cells per unit area was multiplied by total ovary area to give an estimate assuming that all germ cells are equal in size. A correction factor was introduced to take the change in the germ cell nuclear size throughout gestation into account. To generate the correction factor, 20 GCNA-1-labeled cells were randomly selected in a randomly selected section from each ovary, and their mean nuclear diameters were determined by taking 2 separate measurements in each cell with the line measurement application in Northern Eclipse imaging software. The mean nuclear diameter per ovary was calculated and averaged at each gestation age. These values were divided by 5 μm, the thickness of each section, to generate the correction factor for each gestation age. The total number of GCNA-1-labeled cells was divided by the corresponding correction factor to obtain the true estimate: $\hat{Y} = (\bar{y}/\bar{a})A/F$, where: $\hat{Y}$ = total number of GCNA-1 labeled cells in an ovary; $\bar{y} = \Sigma y_i/n$; $\bar{a} = \Sigma a_i/n$; y_i = total number of GCNA-1 labeled cells in ith section; a_i = area of ith section; n = number of sections counted per ovary; A = estimated total area of an ovary; F = correction factor.

To evaluate the precision of the estimates obtained from 5–7 sections of each ovary, we performed metanalyses by recalculating the estimates separately using either 3 or one randomly selected sections from each ovary. In both the main experiment and the metanalyses, 4 ovaries from 4 fetuses from a minimum of 2 litters were examined at each gestation age.

Statistics

Significant differences in the numbers of GCNA-1-labeled cells between gestation ages were assessed by using the Tukey test for multiple pairwise comparisons. All statistical analyses, including mean calculations, were carried out with SYSTAT 9, while SigmaPlot 2000 was used for data presentation (SPSS Science, Chicago, IL).

Results

Comparison of GCNA-1 and MVH immunolabeling in ovaries

Immunolabeling patterns of GCNA-1 and MVH were compared in adjacent sections of ovaries at 15.5 dpc and DOB. Two ovaries from two fetuses from two litters were examined at each gestation age. Biotin–avidin amplification was necessary to obtain labeling with either antibody, and therefore simultaneous detection of the two antigens in the same section was not possible. GCNA-1- and MVH-labeled cells were seen distributed in comparable areas of ovaries. At 15.5 dpc, the labeled cells were distributed evenly throughout the ovary (data not shown), while at DOB they were concentrated in the periphery and scarce in the central region (Fig. 1A and D). No immunolabeling with either antibody was seen in the adjacent mesonephros (data not shown).

At both gestational ages examined, GCNA-1 immunolabeling was localized in the nuclei of a select population of cells, most of which showed the characteristics of the oocyte with spherical shape, large size, and prominent nucleoli

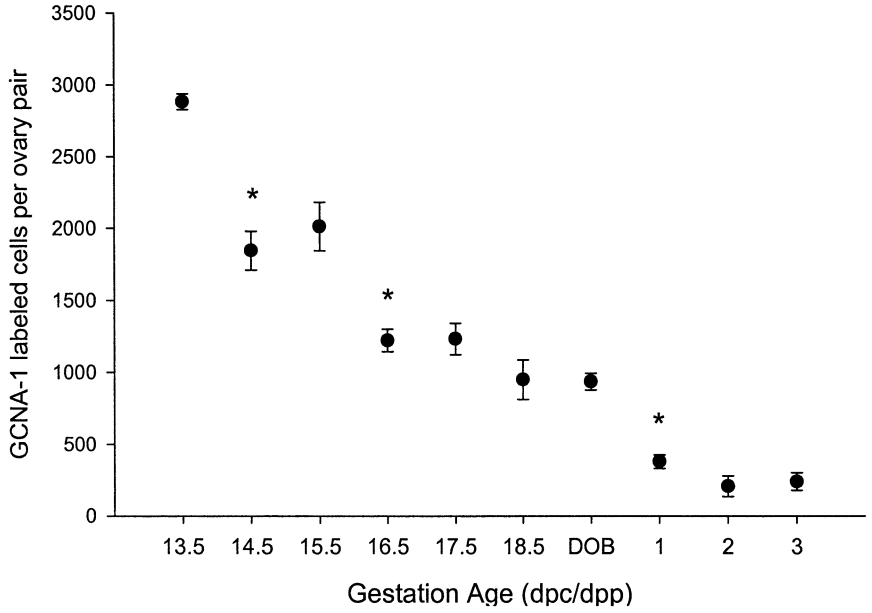

Fig. 4. The total number of GCNA-1-labeled cells recovered from each pair of ovaries by cytospin centrifugation. Each point represents the mean ± SEM obtained from six pairs of ovaries from two litters. Significant decreases are found between 13.5 and 14.5 dpc, between 15.5 and 16.5 dpc, and between DOB and 1 dpp (*, $P < 0.05$).

(Fig. 1B and C). All cells morphologically identified as oocytes with DAPI staining were labeled with the anti-GCNA-1 antibody. In contrast, MVH immunolabeling was seen throughout the cytoplasm of a select population of cells, while it was absent in nuclei as determined by DAPI staining (Fig. 1E and F). All cells morphologically identified as oocytes, again with DAPI staining, were labeled with the anti-MVH antibody. Some cells showed uniform immunolabeling with no corresponding DAPI staining. These were most likely oocytes whose nuclei did not pass through the plane of section. It must be noted that some cells were labeled with either antibody, although they did not show morphological characteristics of oocytes.

Simultaneous immunolabeling with anti-GCNA-1 and anti-MVH antibodies was possible in dispersed ovarian cells since the signal with the anti-GCNA-1 antibody was sufficiently strong without biotin–avidin amplification. The same cell population was labeled with both antibodies, GCNA-1 labeling in the nucleus and MVH labeling in the cytoplasm (Fig. 1G–L). Many cells were faintly labeled with the anti-MVH antibody in the nucleus (Fig. 1H) that was identified by DAPI staining (data not shown) but not in the cytoplasm. None of these cells displayed GCNA-1 labeling. This staining was considered to be nonspecific binding of the anti-MVH antibody in the nucleus of somatic cells.

In all above experiments, ovarian sections or cells incubated in the absence of primary antibodies exhibited no detectable immunolabeling. Similarly, ovarian slides incubated with noncorresponding secondary antibodies exhibited no detectable immunolabeling (data not shown).

Identification of meiotic prophase stages in GCNA-1-labeled cells

We examined whether GCNA-1-positive cells progressed in meiotic prophase during ovarian development by simultaneous labeling with the anti-SC antibody in chromosome spreading preparations. The conventional method yielded a small number of GCNA-1-labeled cells, often fewer than 100, retained on a histological slide. Accordingly, we introduced a cytospin centrifugation step. The numbers of GCNA-1-labeled cells retained on slides increased nearly 10-fold at all gestation ages examined (= 15.5, 16.5, 17.5, and 18.5 dpc) (data not shown). This increase in cell retention greatly facilitated the assay as sufficient numbers of GCNA-1-labeled cells were available in all slides prepared.

Stages of meiotic prophase in GCNA-1-labeled cells were identified by the characteristic patterns of SC labeling (Fig. 2). Leptotene was characterized by diffuse fine thread-like SC immunolabeling throughout the nucleus (Fig. 2B). Early zygotene was characterized by apparent thickening of the threads at discrete loci in the nucleus (Fig. 2D). By mid zygotene, the threads became continuous and fewer in number, but their entire lengths were longer (Fig. 2F). Pachytene was characterized by the presence of 20 discrete threads representing the pairing cores between homologous chromosomes along their entire length (Fig. 2H). Early diplotene was characterized by the appearance of "Y"-shaped or looped SC labeled threads (Fig. 2J). At all stages examined (13.5 to 3 dpp), a population of GCNA-1-labeled cells

showed no detectable SC labeling (Fig. 1L). We named this population "complex negative."

The proportions of GCNA-1-labeled cells at individual meiotic prophase stages were estimated throughout the gestation ages from 13.5 to 3 dpp (Fig. 3). A small population of leptotene oocytes was observed at 13.5 dpc. This population peaked at 14.5 dpc and disappeared by 17.5 dpc, although a small population (3%) reappeared at 18.5 dpc. Zygotene oocytes appeared at 14.5 dpc and peaked at 15.5 dpc. This population persisted and fluctuated between 15.5 and 18.5 dpc and then disappeared by DOB. Pachytene oocytes appeared at 15.5 dpc, and continuously increased to a peak at 17.5 dpc. This population remained elevated until DOB, suddenly dropped to almost none by 1 dpp. Early diplotene oocytes appeared at DOB, peaked at 1 dpp, and declined thereafter. Complex negative oocytes were present at all stages examined. This population was high at 13.5 dpc and rapidly declined with further gestation ages. The population remained low between 15.5 and 18.5 dpc, and then increased thereafter. Few, if any, GCNA-1-negative cells were immunolabeled with the anti-SC antibody.

Changes in the total number of GCNA-1-labeled cells during ovarian development

We estimated the total number of GCNA-1-labeled cells in the chromosome spreading preparation obtained from each pair of ovaries through 13.5 dpc to 3 dpp (Fig. 4). There was a continuous decline in the average number of GCNA-1-labeled cells from 2900 at 13.5 dpc to 250 at 3 dpp. Significant decreases ($P < 0.05$) were found between 13.5 and 14.5 dpc, between 15.5 and 16.5 dpc, and between DOB and 1 dpp.

To verify the biological validity of the decline in the GCNA-1-labeled cell population during fetal development observed in chromosome spreading preparations, we estimated the total number of GCNA-1-labeled cells in the ovary by using the ratio estimation method in histological sections. Changes in the distribution of GCNA-1-labeled cells during ovarian development were apparent upon inspection of histological sections (Fig. 5). At 13.5 dpc, GCNA-1-labeled cells were small in nuclear diameter and clustered throughout the ovary (Fig. 5A). At 15.5 dpc, GCNA-1-labeled cells were still distributed over the ovary; however, they appeared to have larger nuclear diameters and were clustered in larger groups near the periphery (Fig. 5B). At 17.5 dpc, GCNA-1-labeled cells were concentrated toward the periphery, while the size of cell clustering decreased (Fig. 5C). Single cells were more frequently seen in the center. At DOB, the distribution of GCNA-1-labeled cells was similar to that seen at 17.5 dpc; however, the space between the labeled cells appeared to have increased (Fig. 5D). At 2 dpp, GCNA-1-labeled cells were scarce in the center, and the space between the labeled cells appeared to have further increased in the periphery (Fig. 5E).

The measurements made for estimation of the total number of GCNA-1-labeled cells in the ovary are given in Table 1. The average total area of the ovary increased continuously during development with significant differences between 13.5 and 17.5 dpc, as well as between 15.5 dpc and DOB. Meanwhile, the germ cell number per unit area steadily decreased, with significant differences between 15.5 and 17.5 dpc and between 17.5 dpc and DOB. The mean germ cell nuclear diameter increased significantly between 13.5 and 15.5 dpc, as well as between 15.5 and 17.5 dpc.

The final estimates are summarized in Fig. 6A. A steady decrease in the total number of GCNA-1-labeled cells was observed with significant differences at every 2-day interval between 13.5 dpc and DOB ($P < 0.05$). The total number of GCNA-1-labeled cells estimated per ovary ranged from 21171 $\pm$ 673 at 13.5 dpc to 7226 $\pm$ 320 at 2 dpp.

To assess the precision of the estimates obtained from 5–7 randomly selected sections per ovary, the estimates were made similarly but using 3 randomly selected sections or 1 randomly selected section per ovary. Using 3 randomly selected sections per ovary, a constant decrease in the total number of GCNA-1-labeled cells during development was observed (Fig. 6B), similar to the observation made with 5–7 sections per ovary (Fig. 6A). However, significant decreases were found only between 15.5 and 17.5 dpc and between 17.5 dpc and 2 dpp. The total number of GCNA-1-labeled cells per ovary ranged from 20,509 $\pm$ 881 at 13.5 dpc to 7688 $\pm$ 350 at 2 dpp, which are close to the values obtained with 5–7 sections per ovary. An overall decrease in the number of GCNA-1-labeled cells was also observed when only 1 randomly selected section per ovary was used for estimation (Fig. 6C). The number of GCNA-1-labeled cells estimated per ovary ranged from 19,966 $\pm$ 1072 at 13.5 dpc to 7530 $\pm$ 1466 at 2 dpp, which are in the same range as when multiple sections were counted per ovary. However, a significant decrease was observed only between 15.5 and 17.5 dpc, and no loss was found between 13.5 and 15.5 dpc or between 17.5 dpc and 2 dpp.

Discussion

GCNA-1 has advantages as a germ cell marker

Accurate counting of oocytes largely depends on the method used to identify oocytes. Use of biochemical markers is desirable since morphological criteria at the light microscope level are questionable. Indeed, the use of morphology alone to identify oocytes has been pointed out as a potential shortcoming in the previous studies (Baker, 1963; Beaumont and Mandl, 1962). Electron microscopy, while more reliable than light microscopy for defining oocytes, is inadequate for quantification. Despite an abundance of markers for primordial germ cells, very few remain expressed in germ cells throughout ovarian development. Of these, two

Table 1
Measurements in histological sections of ovaries

Gestation age (dpc/dpp)	Total ovary area (mm^2)*	GC nuclear diameter (μm)*	GC number per unit area (μm^2)*	Correction factor**
13.5	0.392 ± 0.025	3.84 ± 0.11	0.0420 ± 0.0029	0.77
15.5	0.469 ± 0.033	4.84 ± 0.19[c]	0.0366 ± 0.0019	0.97
17.5	0.554 ± 0.036[a]	5.84 ± 0.06[d]	0.0278 ± 0.0015[e]	1.17
DOB	0.660 ± 0.056[b]	5.92 ± 0.09	0.0178 ± 0.0006[f]	1.18
1	0.739 ± 0.025	6.08 ± 0.13	0.0133 ± 0.0006	1.22

* Values are expressed as mean ± SEM.
** Correction factor equals mean germ cell (GC) nuclear diameter over 5 μm, thickness of the ovary section.
[a] The increase in total ovary area between 13.5 and 17.5 dpc is significant, $P < 0.05$.
[b] The increase in total ovary area between 15.5 dpc and DOB is significant, $P < 0.05$.
[c] The increase in GC nuclear diameter between 13.5 and 15.5 dpc is significant, $P < 0.05$.
[d] The increase in GC nuclear diameter between 15.5 and 17.5 dpc is significant, $P < 0.05$.
[e] The decrease in GC number per unit area between 15.5 and 17.5 dpc is significant, $P < 0.05$.
[f] The decrease in GC number per unit area between 17.5 dpc and DOB is significant, $P < 0.05$.

antigens, GCNA-1 and MVH, are known to be expressed in oocytes throughout the meiotic prophase (Enders and May, 1994; Toyooka et al., 2000).

In the present study, we compared the immunolabeling patterns of GCNA-1 and MVH in both dispersed cells and histological sections from fetal and neonatal mouse ovaries. All cells labeled for GCNA-1 were also labeled for MVH in ovarian cell suspensions, and a similar population of cells with the characteristics of oocytes was labeled for either antigen in adjacent tissue sections. We conclude that the two markers label the identical population of germ cells. However, we chose GCNA-1 as a better marker for counting oocytes because of its nuclear localization, which was easy to distinguish in both histological sections and ovarian cell suspensions. In contrast, the cytoplasmic labeling of MVH was prone to repeat counting of the same cells, and correction for the increase in oocyte size during ovarian development would have been difficult. Furthermore, hypotonic NaCl treatment of cell suspensions, which was necessary for visualizing SC immunolabeling patterns, destroyed the cytoplasmic integrity of most cells and thus limited the use of MVH immunolabeling.

GCNA-1-labeled cells represent the oocytes that go through meiotic prophase

Simultaneous labeling of GCNA-1 and SC in chromosome spreading preparations revealed that the majority of GCNA-1-labeled cells entered meiosis and progressed through meiotic prophase. The onset as well as the duration of each stage in gestation days corresponded well with those reported in earlier studies (Borum, 1961; Bakken and McClanahan, 1978; Speed, 1982; Dietrich and Mulder, 1983). However, a population of GCNA-1-labeled cells without SC immunolabeling was seen throughout the gestation period examined. This population, termed "complex negative," was high at earlier gestation ages, notably at 13.5 and 14.5 dpc, when most germ cells had yet to enter into meiosis. The majority of these cells are most likely oogonia. Such a "complex negative" cell population decreased rapidly with gestation ages and reached the lowest (<20%) at 18.5 dpc, indicating that the majority of GCNA-1-labeled cells had entered into meiosis. The "complex negative" population increased again at later gestation ages, when synaptonemal complexes began to dissolve as oocytes reached the diplotene stage.

It is unlikely that the small population of "complex negative" GCNA-1-labeled cells observed at 16.5–18.5 dpc entered into meiosis at later developmental stages. First, premeiotic DNA synthesis has been reported to end by 14.5–15.5 dpc in the mouse (Lima-De-Faria and Borum, 1962; Crone et al., 1965; Park and Taketo, unpublished observations). Second, if the GCNA-1-labeled cells were to enter into meiosis at later gestation ages, early meiotic prophase stages would have persisted throughout our profile. This was not observed as leptotene disappeared by 17.5 dpc and zygotene by 18.5 dpc. It is also unlikely that these cells had arrested at early leptotene, which was barely labeled for SC, and resumed meiotic prophase later on since zygotene or pachytene oocytes were not observed after 18.5 dpc.

The "complex negative" GCNA-1-labeled cells observed at 16.5–18.5 dpc may correspond to a population of oogonia arrested in mitosis, which has been recently reported (Wartenburg et al., 2001). Interestingly, these germ cells, maintaining metaphase-like chromosomes but lacking visible spindles, persist without apparent signs of degeneration for as long as 3 days. Assuming that the last premeiotic S-phase occurs at 15.5 dpc, oogonia arrested in mitosis may be seen until 18.5 dpc, as observed in our present studies. The proportion of "arrested oogonia" within the total population of germ cells was not examined in the previous study. Our results suggest that the population of arrested oogonia may be contributing to a significant part of the germ cell loss. We have not excluded other possibilities. For

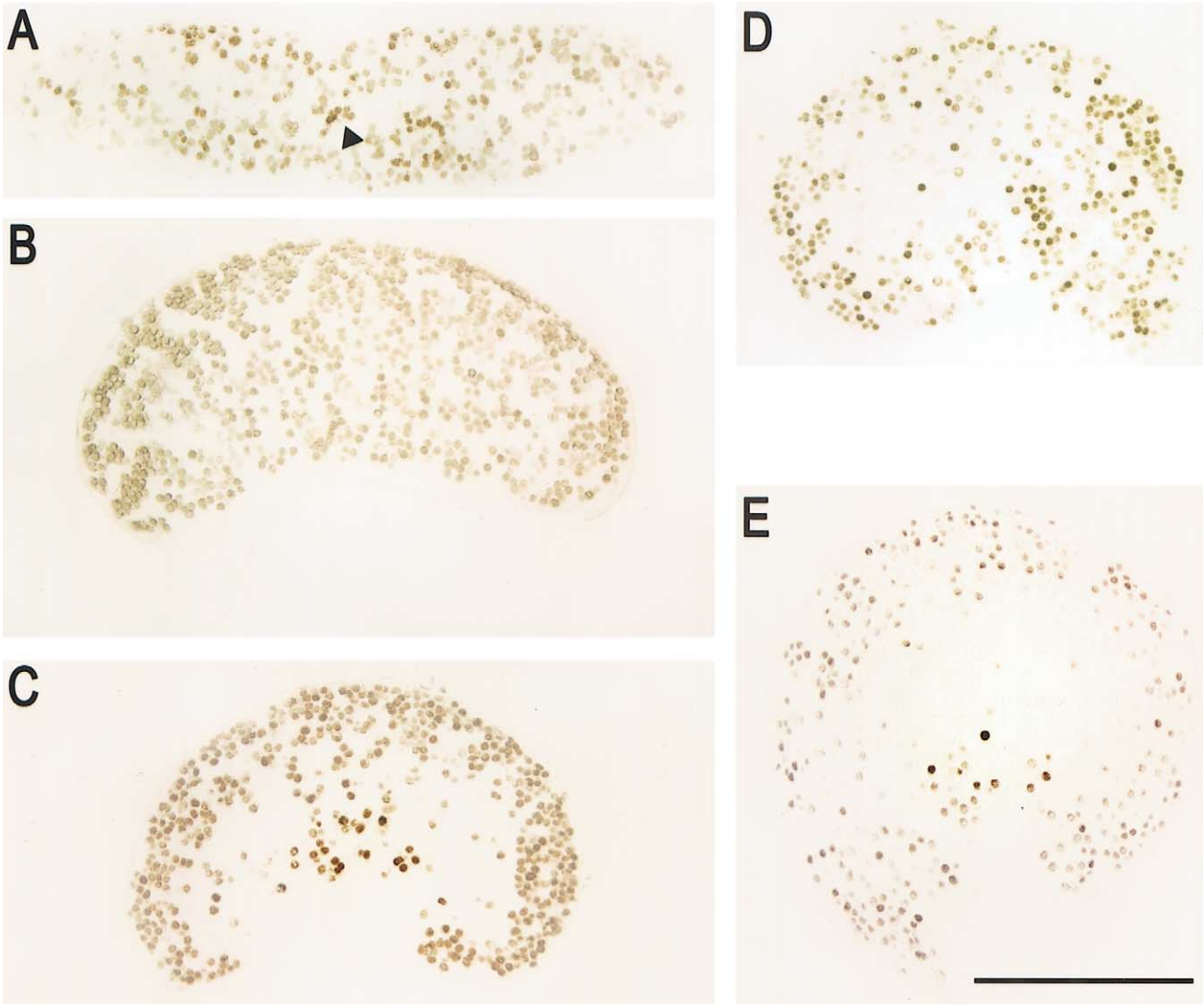

Fig. 5. GCNA-1 labeling in histological sections of fetal (A–C) and neonatal (D, E) ovaries. Scale bar, 250 μm. (A) Mid section of an ovary at 13.5 dpc. The labeled cells are uniformly distributed throughout the ovary. Note the small nuclear diameters and frequent clustering (arrowhead) of the labeled cells. (B) Mid section of an ovary at 15.5 dpc. The labeled cells are distributed throughout the ovary. Note the increased nuclear diameter and larger clustering of labeled cells in the periphery as compared to the section in (A). (C) Mid section in an ovary at 17.5 dpc. The labeled cells are concentrated in the periphery and fewer in the central region. Note less clustering of labeled cells compared with the section in (B). (D) Mid section of an ovary at DOB. Note fewer clustering and increase in the space between the labeled cells in the periphery. (E) Mid section of an ovary at 2 dpp. The labeled cells are seen almost exclusively in the periphery. Note the further increased space between the labeled cells.

example, the "complex negative" GCNA-1-labeled cells may have lost SC antigenicity during cell preparations or represent oocytes undergoing degeneration. Further studies are needed to determine the nature of "complex negative" GCNA-1-labeled cells.

Continuous loss of oocytes during fetal development

The total number of GCNA-1-labeled cells counted in the chromosome spreading preparations indicated a continuous loss of germ cells during fetal development. Significant losses were found between 13.5 and 14.5 dpc, between 15.5 and 16.5 dpc, and between DOB and 1 dpp. These periods correspond to the peak of premeiotic S-phase, the peak of zygotene, and the end of pachytene, respectively. These observations do not support the hypothesis that errors in homologous pairing is the major cause of oocyte loss during meiotic prophase (Speed, 1982). However, the chromosome spreading method used in this study has a technical limitation. Although introduction of a cytospin centrifugation step significantly improved cell retention on slides, the total numbers of GCNA-1-labeled cells counted were far smaller than those previously reported (Tam and Snow, 1981; Jones and Krohn, 1961) or estimated by us in histo-

logical sections. There seemed to be an apparent loss of cells during the isolation process. Furthermore, the loss appears to be exacerbated at later gestation ages if compared with the loss estimated in histological sections. It is conceivable that the oocytes in later stages of meiotic prophase, probably due to their larger sizes, may be more vulnerable to mechanical dissociation or more adhesive to plasticware. Nonetheless, we believe that our results of cytospin chromosome spreading method represent the oocyte population in vivo since the progress and duration of meiotic prophase stages are consistent with the previous reports using histological sections (Borum, 1961; Bakken and McClanahan, 1978; Speed, 1982).

We attempted to make an accurate estimate of the number of germ cells in the ovary by counting the GCNA-1-labeled cells in histological sections and calculating based on the ratio estimation model. We randomly selected sections from each ovary. This is important as it eliminates the possibility of bias when sections are chosen at a particular position or arbitrarily. In addition, we counted multiple sections from each ovary. This increased the accuracy, as discussed below. We also took into consideration the finding that the average germ cell nuclear diameter increased with gestation ages. If we were to simply calculate the total number of germ cells based on the number per section and total ovary area, the estimates would have been deflated at earlier ages since the average nuclear diameter is smaller than the thickness of one section. As well, the estimates would have been inflated at later gestation ages since the average nuclear diameter is larger than the thickness of one section.

The results from histological sections are consistent with those obtained with cell suspensions, indicating a continuous loss of germ cells during fetal development. Significant loss was seen at every 2-day interval examined except for the period between DOB and 2 dpp. These results agree with earlier studies (Borum, 1961; Bakken and McClanahan, 1978; Speed, 1982). Furthermore, we found the loss of germ cells from 13.5 dpc to DOB to be approximately 65%. This result is in agreement with the percentage loss observed in the rat and human (Beaumont and Mandl, 1962; Baker, 1963).

On the other hand, our present results as well as many previous reports disagree with the study using MVH as a germ cell marker (Pepling and Spradling, 2000). The latter authors did not find any loss of oocytes in fetal life but found a major loss between 1 and 2 dpp. Furthermore, the total numbers of germ cells estimated, ranging from 6000 at 13.5 dpc to 2000 after birth, are much smaller than the estimates obtained by others including ourselves. This discrepancy cannot be simply attributed to different markers to identify oocytes since our results showed that the 2 markers label identical germ cell populations. Possible recounting of the same cells due to cytoplasmic labeling may inflate the estimate but cannot explain the underestimation. Nor can the discrepancy be explained by differences between mouse strains as both studies used CD-1 mice. We believe that the discrepancy arose due to different methods of oocyte counting. Pepling and Spradling counted the total MVH-labeled cells in a single representative section from each ovary. Using the average diameter of a germ cell, the fraction of ovarian volume represented by the counted section was calculated. This allowed for the computation of the total number of germ cells in the whole ovary. This counting method was modified at 21.5 dpc and later to take into account the differences in germ cell density in the inner and outer cortex, although no details of the modification were provided. It must be noted that this gestation age coincides with the abrupt decrease in the number of oocytes found by the authors. Also, Burgoyne and Baker (1985) have pointed out that errors may occur by selecting the area for counting in perinatal ovaries when the distribution of germ cells is not random and the oocytes at the diplotene stage vary enormously in size. We believe that counting all cells in multiple randomly selected sections gives the best estimate in such a case.

The number of sections counted per ovary affects the accuracy

For the sake of accuracy, we counted multiple (5–7) sections, covering 10% of the total number of sections, from each ovary. To evaluate the need for such a rigorous counting method to estimate the total germ cell population, we recalculated the estimates based on three and one randomly selected section per ovary. The results were similar when only three sections were counted per ovary. However, statistical significance was lost at certain points probably as a result of counting a small number of ovaries. Quite different results were obtained when only single section was counted per ovary. Although the overall trend of germ cell loss was observed and the range of germ cell numbers was similar to those obtained with multiple sections, no losses were observed at many intervals of ovarian development. These results further justify the need for counting multiple sections per ovary.

Conclusions

We have shown that the oocyte population continuously decreased during meiotic prophase in the mouse ovary. This observation does not favor any one particular cause of germ cell elimination. Instead, it suggests the involvement of multiple causes, probably including the need for trophic factors, errors in mitosis and chromosome pairing, or telomere defects. The method established here is useful for identifying the stage of meiotic prophase at which oocytes undergo major degeneration due to genetic mutations or sex chromosome anomalies.

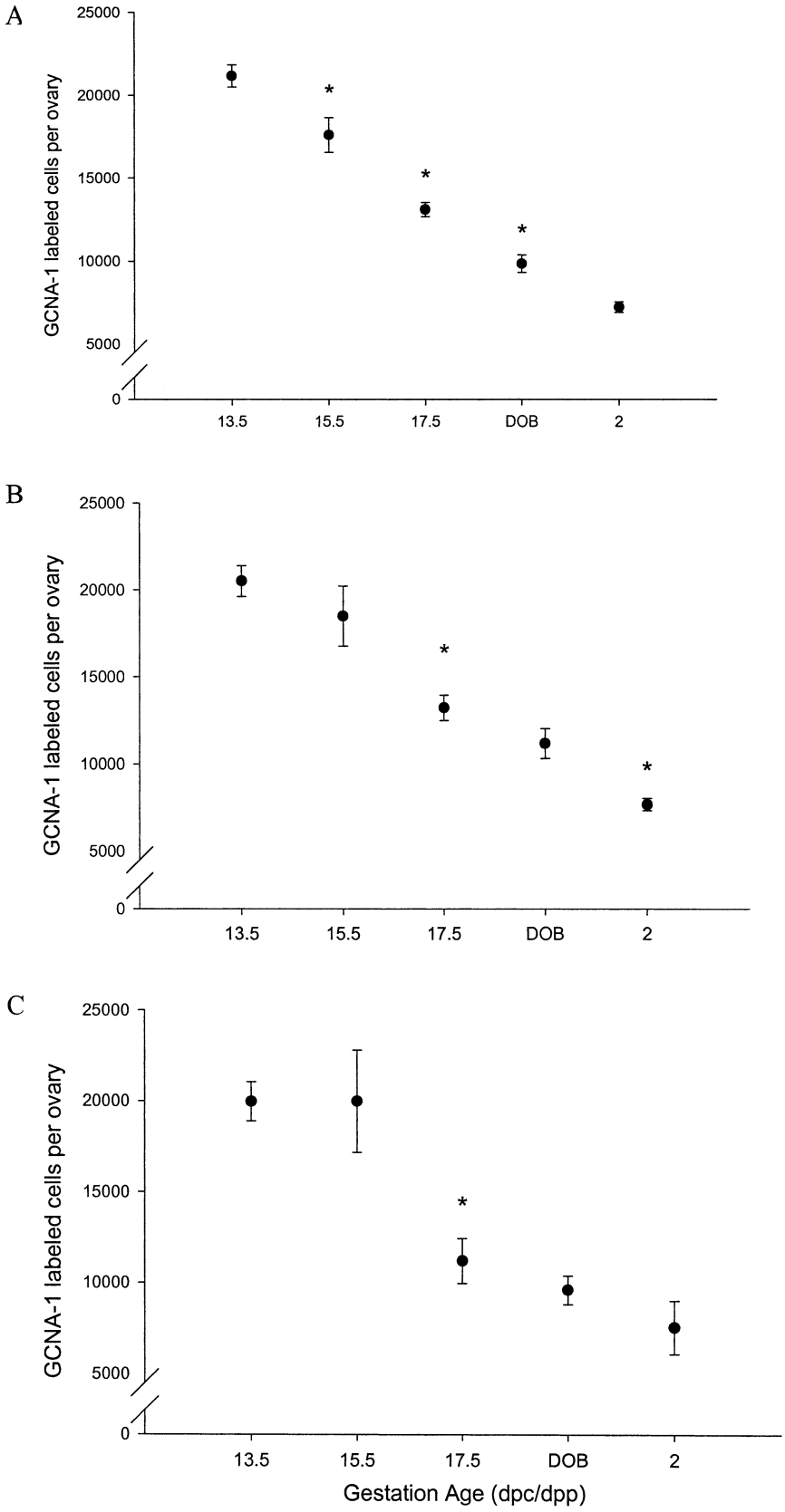

Fig. 6. Changes in the total number of GCNA-1-labeled cells in the ovary during development estimated in histological sections. (A) The number of GCNA-1-labeled cells counted in 5–7 randomly selected sections from each ovary. Each value represents the mean ± SEM of 4 ovaries from two litters. Significant decreases are found in all intervals examined (*, $P < 0.05$) except for the interval between DOB and 2 dpp. (B) The number of GCNA-1-labeled cells counted in 3 randomly selected sections from each ovary. Each value represents the mean ± SEM of 4 ovaries from two litters. Significant decreases are found between 15.5 and 17.5 dpc and between 17.5 dpc and 2 dpp (*, $P < 0.05$). (C) The number of GCNA-1-labeled cells counted in 1 randomly selected section from each ovary. Each value represents the mean ± SEM of 4 ovaries from two litters. Significant decrease is found between 15.5 and 17.5 dpc (*, $P < 0.05$).

Acknowledgments

We thank Drs. G.C. Enders (University of Kansas, Kansas City, KS), T. Noce (Mitsubishi-Kasei Institute of Life Sciences, Tokyo, Japan), and P. Moens (York University, Toronto, ON) for the gifts of antibodies against GCNA-1, MVH, and SC, respectively. We also thank Mr. F. Rouah and Dr. K. Worsely (Department of Mathematics and Statistics, McGill University) for their help with statistical analyses. This study was supported by a CIHR grant (to T.T.).

References

Amleh, A., Smith, L., Chen, H., Taketo, T., 2000. Both nuclear and cytoplasmic components are defective in oocytes of the B6.Y^{TIR} sex-reversed female mouse. Dev. Biol. 219, 277–286.

Baker, S.M., Plug, A.W., Prolla, T.A., Bronner, C.E., Harris, A.C., Yao, X., Christie, D.-M., Monell, C., Arnheim, N., Bradley, A., Ashley, T., Liskay, R.M., 1996. Involvement of mouse Mlh1 in DNA mismatch repair and meiotic crossing over. Nat. Genet. 13, 336–342.

Baker, T.G., 1963. A quantitative and cytological study of germ cells in human ovaries. Proc. R. Soc. Lond. B Biol. Sci. 158, 417–433.

Baker, T.G., Franchi, L.L., 1967. The fine structure of oogonia and oocytes in human ovaries. J. Cell Sci. 2, 213–224.

Bakken, A.H., McClanahan, M., 1978. Patterns of RNA synthesis in early meiotic prophase oocytes from fetal mouse ovaries. Chromosoma 67, 21–40.

Beaumont, H.M., Mandl, A.M., 1962. A quantitative and cytological study of oogonia and oocytes in the foetal and neonatal rat. Proc. R. Soc. Lond. B. Biol. Sci. 155, 557–579.

Borum, K., 1961. Oogenesis in the mouse: a study of the meiotic prophase. Exp. Cell Res. 24, 495–507.

Brannan, C.I., Lyman, S.D., Williams, D.E., Eisenman, J., Anderson, D.M., Cosman, D., Bedell, M.A., Jenkins, N.A., Copeland, N.G., 1991. Steel-Dickie mutation encodes a c-Kit ligand lacking transmembrane and cytoplasmic domains. Proc. Natl. Acad. Sci. USA 88, 4671–4674.

Burgoyne, P.S., Baker, T.G., 1985. Perinatal oocyte loss in XO mice and its implications for the aetiology of gonadal dysgenesis in XO women. J. Reprod. Fertil. 75, 633–645.

Burgoyne, P.S., Mahadevaiah, S., Mittwoch, U., 1985. A reciprocal autosomal translocation which causes male sterility in the mouse also impairs oogenesis. J. Reprod. Fertil. 75, 647–652.

Chabot, B., Stephenson, D.A., Chapman, V.M., Besmer, P., Bernstein, A., 1988. The proto-oncogene c-kit encoding a transmembrane tyrosine kinase receptor maps to the mouse W locus. Nature 335, 88–89.

Crone, M., Levy, E., Peters, H., 1965. The duration of the premeiotic DNA synthesis in mouse oocytes. Exp. Cell Res. 39, 678–688.

Dietrich, A.J.J., Mulder, R.J.P., 1983. A light and electron microscopic analysis of meiotic prophase in female mice. Chromosoma 88, 377–385.

Dobson, M.J., Pearlman, R.E., Karaiskakis, A., Spyropoulos, B., Moens, P.B., 1994. Synaptonemal complex proteins: occurrence, epitope mapping and chromosome disjunction. J. Cell Sci. 107, 2749–2760.

Dolci, S., Pesce, M., De Felici, M., 1993. Combined action of stem cell factor, leukemia inhibitory factor, and cAMP on in vitro proliferation of mouse primordial germ cells. Mol. Reprod. Dev. 35, 134–139.

Edelmann, W., Cohen, P.E., Kneitz, B., Winand, N., Lia, M., Heyer, J., Kolodner, R., Pollard, J.W., Kucherlapati, R., 1999. Mammalian MutS homologue 5 is required for chromosome pairing in meiosis. Nat. Genet. 21, 123–127.

Edelmann, W., Cohen, P.E., Kane, M., Lau, K., Morrow, B., Bennett, S., Umar, A., Kunkel, T., Cattoretti, G., Chaganti, R., Pollard, J.W., Kolodner, R.D., Kucherlapati, R., 1996. Meiotic pachytene arrest in MLH1-deficient mice. Cell 85, 1125–1134.

Enders, G.C., May 2nd, J.J., 1994. Developmentally regulated expression of a mouse germ cell nuclear antigen examined from embryonic day 11 to adult in male and female mice. Dev. Biol. 163, 331–340.

Franchi, L.L., Mandl, A.M., 1962. The ultrastructure of oogonia and oocytes in the foetal and neonatal rat. Proc. R. Soc. Lond. B Biol. Sci. 157, 99–114.

Fujiwara, Y., Komiya, T., Kawabata, H., Sato, M., Fujimoto, H., Furusawa, M., Noce, T., 1994. Isolation of a DEAD-family protein gene that encodes a murine homolog of Drosophila vasa and its specific expression in germ cell lineage. Proc. Natl. Acad. Sci. USA 91, 12258–12262.

Godin, I., Deed, R., Zsebo, K., Dexter, M., Wylie, C.C., 1991. Effects of the steel gene product on mouse primordial germ cells in culture. Nature 352, 807–811.

Hemann, M.T., Rudolph, K.L., Strong, M.A., DePinho, R.A., Chin, L., Greider, C.W., 2001. Telomere dysfunction triggers developmentally regulated germ cell apoptosis. Mol. Biol. Cell 12, 2023–2030.

Heyting, C., Dettmers, R.J., Dietrich, A.J., Redeker, E.J., Vink, A.C., 1988. Two major components of synaptonemal complexes are specific for meiotic prophase. Chromosoma 96, 325–332.

Huang, E., Nocka, K., Beier, D.R., Chu, T.-Y., Buck, J., Lahm, H.-W., Wellner, D., Leder, P., Besmer, P., 1990. The hematopoietic growth factor KL is encoded by the S1 locus and is the ligand of the c-kit receptor, the gene product of the X locus. Cell 63, 225–233.

Jones, E.C., Krohn, P.L., 1961. The relationships between age, numbers of oocytes and fertility in virgin and multiparous mice. J. Endocrinol. 21, 469–495.

Kneitz, B., Cohen, P.E., Avdievich, E., Zhu, L., Kane, M.F., Hou Jr., H., Kolodner, R.D., Kucherlapati, R., Pollard, J.W., Edelmann, W., 2000. MutS homolog 4 localization to meiotic chromosomes is required for chromosome pairing during meiosis in male and female mice. Genes Dev. 14, 1085–1097.

Koshimizu, U., Watanabe, M., Nakatsuji, N., 1995. Retinoic acid is a potent growth activator of mouse primordial germ cells in vitro. Dev. Biol. 168, 683–685.

Levy, P.S., Lemeshow, S., 1999. Ratio estimation, in: Levy, P.S., Lemeshow, S. (Eds.), Sampling of Populations: Methods and Applications, John Wiley & Sons, New York, pp. 191–224.

Lima-De-Faria, A., Borum, K., 1962. The period of DNA synthesis prior to meiosis in the mouse. J. Cell Biol. 14, 381–388.

Matsui, Y., Toksoz, D., Nishikawa, S., Nishikawa, S., Williams, D., Zsebo, K., Hogan, B.L.M., 1991. Effect of Steel factor and leukaemia inhibitory factor on murine primordial germ cells in culture. Nature 353, 750–752.

Mintz, B., Russell, E.S., 1957. Gene-induced embryological modifications of primordial germ cells in the mouse. J. Exp. Zool. 134, 207–237.

Mittwoch, U., Mahadevaiah, S.K., 1992. Unpaired chromosomes at meiosis: cause or effect of gametogenic insufficiency? Cytogenet. Cell Genet. 59, 274–279.

Morita, Y., Tilly, J.L., 1999. Segregation of retinoic acid effects on fetal ovarian germ cell mitosis versus apoptosis by requirement for new macromolecular synthesis. Endocrinology 140, 2696–2703.

Pepling, M.E., Spradling, A.C., 2001. Mouse ovarian germ cell cysts undergo programmed breakdown to form primordial follicles. Dev. Biol. 234, 339–351.

Pesce, M., Farrace, M.G., Piacentini, M., Dolci, S., De Felici, M., 1993. Stem cell factor and leukemia inhibitory factor promote primordial germ cell survival by suppressing programmed cell death (apoptosis). Development 118, 1089–1094.

Pesce, M., Wang, X., Wolgemuth, D.J., Scholer, H., 1998. Differential expression of the Oct-4 transcription factor during mouse germ cell differentiation. Mech. Dev. 71, 89–98.

Pittman, D.L., Cobb, J., Schimenti, K.J., Wilson, L.A., Cooper, D.M., Brignull, E., Handel, M.A., Schimenti, J.C., 1998. Meiotic prophase

arrest with failure of chromosome synapsis in mice deficient for Dmc1, a germline-specific RecA homolog. Mol. Cell 1, 697–705.

Resnick, J.L., Bixler, L.S., Cheng, L., Donovan, P.J., 1992. Long-term proliferation of mouse primordial germ cells in culture. Nature 359, 550–551.

Schalk, J.A., Dietrich, A.J., Vink, A.C., Offenberg, H.H., van Aalderen, M., Heyting, C., 1998. Localization of SCP2 and SCP3 protein molecules within synaptonemal complexes of the rat. Chromosoma 107, 540–548.

Speed, R.M., 1982. Meiosis in the foetal mouse ovary. I. An analysis at the light microscope level using surface-spreading. Chromosoma 85, 427–437.

Speed, R.M., 1988. The possible role of meiotic pairing anomalies in the atresia of human fetal oocytes. Hum. Genet. 78, 260–266.

Tam, P.P., Snow, M.H., 1981. Proliferation and migration of primordial germ cells during compensatory growth in mouse embryos. J. Embryol. Exp. Morphol. 64, 133–147.

Tilly, J.L., 2001. Commuting the death sentence: how oocytes strive to survive. Nat. Rev. Mol. Cell Biol. 2, 838–848.

Toyooka, Y., Tsunekawa, N., Takahashi, Y., Matsui, Y., Satoh, M., Noce, T., 2000. Expression and intracellular localization of mouse Vasa-homologue protein during germ cell development. Mech. Dev. 93, 139–149.

Wang, D., Ikeda, Y., Parker, K.L., Enders, G.C., 1997. Germ cell nuclear antigen (GCNA1) expression does not require a gonadal environment or steroidogenic factor 1: examination of GCNA1 in ectopic germ cells and in Ftz-F1 null mice. Mol. Reprod. Dev. 48, 154–158.

Wartenberg, H., Ihmer, A., Schwarz, S., Miething, A., Viebahn, C., 2001. Mitotic arrest of female germ cells during prenatal oogenesis. A colcemid-like, non-apoptotic cell death. Anat. Embryol. 204, 421–435.

Zsebo, K.M., Williams, D.A., Geissler, E.N., Broudy, V.C., Martin, F.H., Atkins, H.L., Hsu, R., Birkett, N.C., Okino, K.H., Murdock, D.C., Jacobsen, F.W., Langley, K.E., Smith, K.A., Takeishi, T., Cattanach, B.M., Galli, S.J., Suggs, S.V., 1990. Stem cell factor is encoded at the S1 locus of the mouse and is the ligand for the c-kit tyrosine kinase receptor. Cell 63, 213–224.